British Journal of Pharmacology

British Journal of Pharmacology (2017) **174** 254–266 254

RESEARCH PAPER

Clemizole hydrochloride blocks cardiac potassium currents stably expressed in HEK 293 cells

Correspondence Dr Yan Wang and Dr Gui-Rong Li, Xiamen Cardiovascular Hospital, Xiamen University, Xiamen, Fujian, 361004 China. E-mail: wy@medmail.com.cn; grli8@outlook.com

Received 3 January 2016; **Revised** 21 November 2016; **Accepted** 22 November 2016

Ling-Jun Jie[1]*, Wei-Yin Wu[1]*, Gang Li[1], Guo-Sheng Xiao[1], Shetuan Zhang[2], Gui-Rong Li[1] and Yan Wang[1]

[1]Xiamen Cardiovascular Hospital, Xiamen University, Xiamen, China, and [2]Department of Biomedical and Molecular Sciences, Queen's University, Kingston, Canada

*These two authors contributed equally to this work.

BACKGROUND AND PURPOSE

Clemizole, a histamine H_1 receptor antagonist has a potential therapeutic effect on hepatitis C infection and also potently inhibits TRPC5 ion channels. The aim of the present study was to investigate whether clemizole blocks cardiac K^+ currents and thus affects cardiac repolarization.

EXPERIMENTAL APPROACH

Whole-cell patch techniques was used to examine the effects of clemizole on hERG channel current, I_{Ks} and $K_v1.5$ channel current in HEK 293 cell expression systems as well as on ventricular action potentials of guinea pig hearts. Isolated hearts from guinea pigs were used to determine the effect on the ECG.

KEY RESULTS

Clemizole decreased hERG current by blocking both open and closed states of the channel in a concentration-dependent manner (IC_{50}: 0.07 μM). The S631A, S636A, Y652A and F656V hERG mutant channels reduced the inhibitory effect of clemizole (IC_{50}: 0.82, 0.89, 1.49 and 2.98 μM, respectively), suggesting that clemizole is a pore blocker of hERG channels. Clemizole also moderately decreased I_{Ks} and human $K_v1.5$ channel current. Moreover, clemizole increased the duration of the ventricular action potential in guinea pig hearts and the QTc interval in isolated perfused hearts from guinea pigs, in a concentration-dependent manner (0.1–1.0 μM).

CONCLUSION AND IMPLICATIONS

Our results provide the first evidence that clemizole potently blocks hERG channels, moderately inhibits cardiac I_{Ks}, delays cardiac repolarization and thereby prolongs QT interval. Thus, caution should be taken when clemizole is used as a TRPC5 channel blocker or for treating hepatitis C infection.

Abbreviations

APD, action potential duration; hERG, human ether-à-go-go-related gene K^+ channel; I_{Kr}, rapidly activating delayed rectifier K^+ current; I_{Ks}, slowly activating delayed rectifier K^+ current; I_{Kur}, ultra-rapidly activating delayed rectifier K^+ current; QTc interval, corrected QT interval

DOI:10.1111/bph.13679

Tables of Links

TARGETS
Voltage-gated ion channels
K_v11.1 (hERG) channels
K_v7.1 (I_{Ks}) channels
K_v1.5 channels

LIGANDS
Clemizole

These Tables list key protein targets and ligands in this article which are hyperlinked to corresponding entries in http://www.guidetopharmacology.org, the common portal for data from the IUPHAR/BPS Guide to PHARMACOLOGY (Southan *et al.,* 2016), or PubChem. Entries from the Guide to PHARMACOLOGY are permanently archived in the Concise Guide to PHARMACOLOGY 2015/16 (Alexander *et al.,* 2015).

Introduction

Clemizole [1-p-chlorobenzyl-2-(1-pyrrolidinyl) methylbenzimidazole] is a histamine H_1-receptor antagonist used to treat allergic reactions and dermal diseases (Finkelstein *et al.,* 1960; Jacques and Fuchs, 1960; Wansker, 1962). Although clemizole is not currently used clinically as a single-agent antihistamine, attention has been paid, recently, to its new therapeutic potential for treating hepatitis C virus (HCV) infection, via inhibiting the binding of NS4B to RNA of HCV (Einav *et al.,* 2008) and for the rare but severe genetic disease, Dravet syndrome (Baraban *et al.,* 2013). Moreover, clemizole strongly inhibits the TRPC5 cation channels (Richter *et al.,* 2014). However, the effects of clemizole on other ionic currents are not understood, especially the K^+ currents involved in cardiac repolarization.

Human *ether-à-go-go*-related gene (hERG or *KCNH2*) encodes the α-subunit of channel conducting the the rapidly activating delayed rectifier potassium current (I_{Kr}) that contributes importantly to the repolarization of cardiac action potentials in humans. Dysfunction of I_{Kr} induces long QT syndrome that predisposes affected individuals to life-threatening arrhythmias. In addition to inherited mutations of hERG, a variety of drugs can impair hERG function, causing long QT syndrome (Sanguinetti and Tristani-Firouzi, 2006; Vandenberg *et al.,* 2012). The present study examined the effect of clemizole on stably expressed hERG channels, slowly activating delayed rectifier potassium current (I_{Ks}) (hKCNE1/hKCNQ1) and hK_v1.5 channels in HEK 293 cells and its effect on cardiac repolarization in guinea pig ventricular myocytes and perfused hearts *ex vivo*. We found that clemizole not only potently blocked hERG channels, but also inhibited hKCNQ1/hKCNE1 and hK_v1.5 channel currents. It increased ventricular action potential duration (APD) and prolonged the corrected QT interval (QTc interval) of the ECG in isolated perfused hearts.

Methods

Cell culture and plasmid transfection

The HEK 293 cell line (Zhang *et al.,* 2010) stably expressing hERG (K_v11.1 or *KCNH2*) or hK_v1.5 (*KCN5A*) channels was maintained in DMEM (Hyclone, Shanghai, China) with 400 μg·mL^{-1} G418 (Sangon Biotech, Shanghai, China) and 10% FBS. HEK 293 cell line stably expressing hKCNQ1/hKCNE1 channels (I_{Ks}) was cultured in DMEM containing 100 μg·mL^{-1} hygromycin B (Invitrogen, Hong Kong, China) and 10% FBS. Cells used for electrophysiology were seeded on glass coverslips.

The hERG mutants F656V, Y652A, S631A and S636A in pcDNA3 vector (Tang *et al.,* 2008; Zhang *et al.,* 2010) were transfected into HEK 293 cells in 12-well plates using 6 μL of Lipofectamine 2000 with 3.5 μg of plasmids. Thirty-six to 48 h after transfection, the transfected cells were used for pharmacological studies.

Preparation of guinea pig cardiomyocytes and ex vivo hearts

All animal care and experimental procedures were approved by the Institutional Ethics Committee of Animal Use for Teaching and Research. Animal studies are reported in compliance with the ARRIVE guidelines (Kilkenny *et al.,* 2010; McGrath and Lilley, 2015). Dunkin-Hartley guinea pigs of either sex ((250-300 g), from the Shanghai Laboratory Research Center (Shanghai, China) were used in this study. The animals were housed (3 per cage) under conditions of controlled temperature (23-25°C) and humidity (55-65%) with a 12-h light/dark cycle. The animals had *ad libitum* access to water and food. The animals were randomly grouped and anaesthetized with sodium pentobarbital (60 mg·kg^{-1}, i.p.) for cardiac cell isolation or *ex vivo* heart study. For cardiac cell isolation, the heart was perfused and then its ventricular myocytes were enzymically dissociated as described previously (Li *et al.,* 2002; Liu *et al.,* 2007). The isolated cardiomyocytes were maintained in a high-K^+ storage medium (composition in mM): KCl 10, K-glutamate 120, KH_2PO_4 10, 1.8 $MgSO_4$ 1.8, taurine 10, HEPES 10, EGTA 0.5, glucose 20, mannitol 10, pH adjusted to 7.3 with KOH) at room temperature for 2 h before electrophysiological recording.

For the *ex vivo* heart study, the isolated heart was perfused with Krebs–Henseleit solution (composition in mM): NaCl 118.3, KCl 4.74, $CaCl_2$ 2.5, KH_2PO_4 1.2, $MgSO_4$ 1.2, glucose 10, $NaHCO_3$ 25; pH adjusted to 7.4 with NaOH), warmed to 37°C and gassed with 95% O_2 and 5% CO_2, as described previously (Liu *et al.,* 2010). Briefly, after the animals were anaesthetized, as described above, their hearts were rapidly excised, mounted in a Langendorff system and retrogradely perfused with a pressure of 70 cm H_2O. Polyethylene tubing

with a deflated water balloon connected to a pressure transducer was inserted into the left ventricle through a small incision in the left atrium to measure left ventricular systolic pressure (LVSP) and contraction/relaxation velocity (±dP/dT). The ECG was recorded with two electrodes placed on the apex and the base of the heart surface (Liu *et al.,* 2010) during the experiments. Hearts with severe cardiac arrhythmias (i.e. frequent ventricular premature beats or ventricular fibrillation >2 min) were excluded from further continuous experiment or data analysis.

The biological signals were recorded using a digital recording system (RM6240, Chengdu Instruments, Chengdu, China) and analysed offline. The QTc interval was calculated with Van de Water's formula (Van de Water *et al.,* 1989): QTc = QT − 0.087 × (RR − 1000). This correction formula showed good correlation of QT interval with the cardiac repolarization period (Takahara *et al.,* 2005; Morissette *et al.,* 2015). After stabilization for 30 min, clemizole was added to the perfusion medium, and its effect on QTc interval was examined.

Electrophysiology

A whole-cell patch clamp technique was employed to record membrane current in voltage-clamp mode and action potentials in current-clamp mode with an EPC-10 amplifier and pulse software (HEKA; Lambercht, Göttingen, Germany) as described previously (Zhang *et al.,* 2008; Liu *et al.,* 2010). Borosilicate glass electrodes (OD 1.2 mm) were pulled with a Brown-Flaming puller (Model P-97; Sutter Instrument Co., Novato, USA) and had resistances of 1.5–2.5 MΩ when filled with the pipette solution. A 2-M KCl-agar bridge was used as the reference electrode. The potential of the pipette tip was zeroed before the pipette touched the cell. After obtaining a gigaohm seal, the membrane patch was ruptured by a gentle suction to establish a whole-cell configuration. Series resistance (R_s) was compensated by 70–80% to minimize voltage errors. The liquid junction potential (14.3 mV) between pipette solution and bath solution, calculated with the software Clampex, was not corrected during the experiment and was corrected for during analysis of the effects of clemizole on voltage-dependent parameters of the ion channel currents, as specified in the Results and Figure legends. Electrical signals were stored on the hard disk of a Dell computer. Current recordings were conducted at room temperature (22–24°C) and action potential recordings were conducted at 36–37°C. Cells with unstable R_s during drug administration were excluded from data analysis.

Data and statistical analysis

The data and statistical analysis in this study comply with the recommendations on experimental design and analysis in pharmacology (Curtis *et al.*, 2015). Data were expressed as mean ± SEM. Statistical comparisons were evaluated with paired or unpaired Student's *t*-test and with repeated measures ANOVA, as appropriate, followed by the Newman–Keuls test. Non-linear curve fitting was performed using Pulsefit (HEKA) and/or Sigmaplot (SPSS Science, Chicago, IL, USA). A value of $P < 0.05$ was considered significant.

Materials

Tyrode's solution contained (in mM): NaCl 140, KCl 5.0, $MgCl_2$ 1.0, $CaCl_2$ 1.8, NaH_2PO_4 0.33, HEPES 10.0, glucose 10 and pH adjusted to 7.3 with NaOH. The pipette solution contained (in mM): KCl 20, K-aspartate 110, HEPES 10, EGTA 5.0 and GTP 0.1, Na_2-phosphocreatine 5.0, MgATP (or K_2-ATP for I_{Ks} or action potential recording) 5.0, with pH adjusted to 7.2 with KOH. Clemizole chloride (Tocris, Bristol, UK) was dissolved in DMSO (Sigma-Aldrich, St Louis, MO, USA).

Results

Clemizole inhibits hERG channels

Figure 1A shows the time-dependent effect of clemizole on tail current through hERG channels ($I_{hERG.tail}$), recorded in a representative hERG-expressing cell with the original voltage protocol without correcting liquid junctional potential) as shown in the inset (a voltage step to +50 mV for 3 s from a holding potential of −80 mV, then to −50 mV). Clemizole at 0.1 μM in bath solution gradually inhibited the current, and the inhibitory effect was partly reversed by washout for 10 min.

Figure 1B demonstrates the family of I_{hERG} upon various depolarization voltages before (control) and after application of 0.1 μM clemizole. Figure 1C illustrates the current–voltage (*I–V*) relationships of hERG current before and after 0.03, 0.1 and 0.3 μM clemizole, the voltage range (−54.3 mV to +45.7 mV) post-corrected for the liquid junction potential. Both $I_{hERG.step}$ and $I_{hERG.tail}$ were reduced by clemizole in a concentration-dependent manner ($n = 8$, $P < 0.05$ vs. control). Figure 1D shows that clemizole-mediated hERG blockade was not voltage dependent. Figure 1E illustrates that the current activation variables (normalized $I_{hERG.tail}$) of hERG channels were fitted to a Boltzmann distribution. The half activation potential ($V_{0.5}$) was not altered by 0.1 μM clemizole (−12.7 ± 1.6 mV for control; −16.4 ± 1.9 mV for clemizole, $n = 7$, $P > 0.05$).

The blockade by clemizole of the hERG channels was examined using four hERG mutants: S631A, S636A, Y652A and F656V. The S636 and S631 residues are on the pore helix of the channels and the alanine mutants exhibit decreased channel inactivation. These mutant channels are generally used for determining the role of inactivation in hERG channel blocking (Zhang *et al.,* 1999; Guo *et al.,* 2006). The F656V and Y652A mutants, in the S6 region, are reported to attenuate hERG channel blockade by several drugs, as these sites constitute the binding site for various drugs (Su *et al.,* 2004; Zhang *et al.,* 2010). These hERG mutants were therefore used in the present study to analyse the potential molecular determinants of clemizole binding.

Figure 2A depicts the wild-type hERG (WT-hERG) and mutant currents recorded in a voltage step as shown in the inset before (control) and after application of 1 μM clemizole. WT-hERG current was almost completely inhibited by clemizole. However, the currents carried by the S631A, F656V and Y652A channels were only partly inhibited by clemizole. The deactivation of F656V current was clearly facilitated by clemizole, which was not observed in WT, S631A or F656V channels. Figure 2B summarises the effects of 1 μM clemizole as an inhibitor of $I_{hERG.tail}$ current, in the WT and mutant channels.

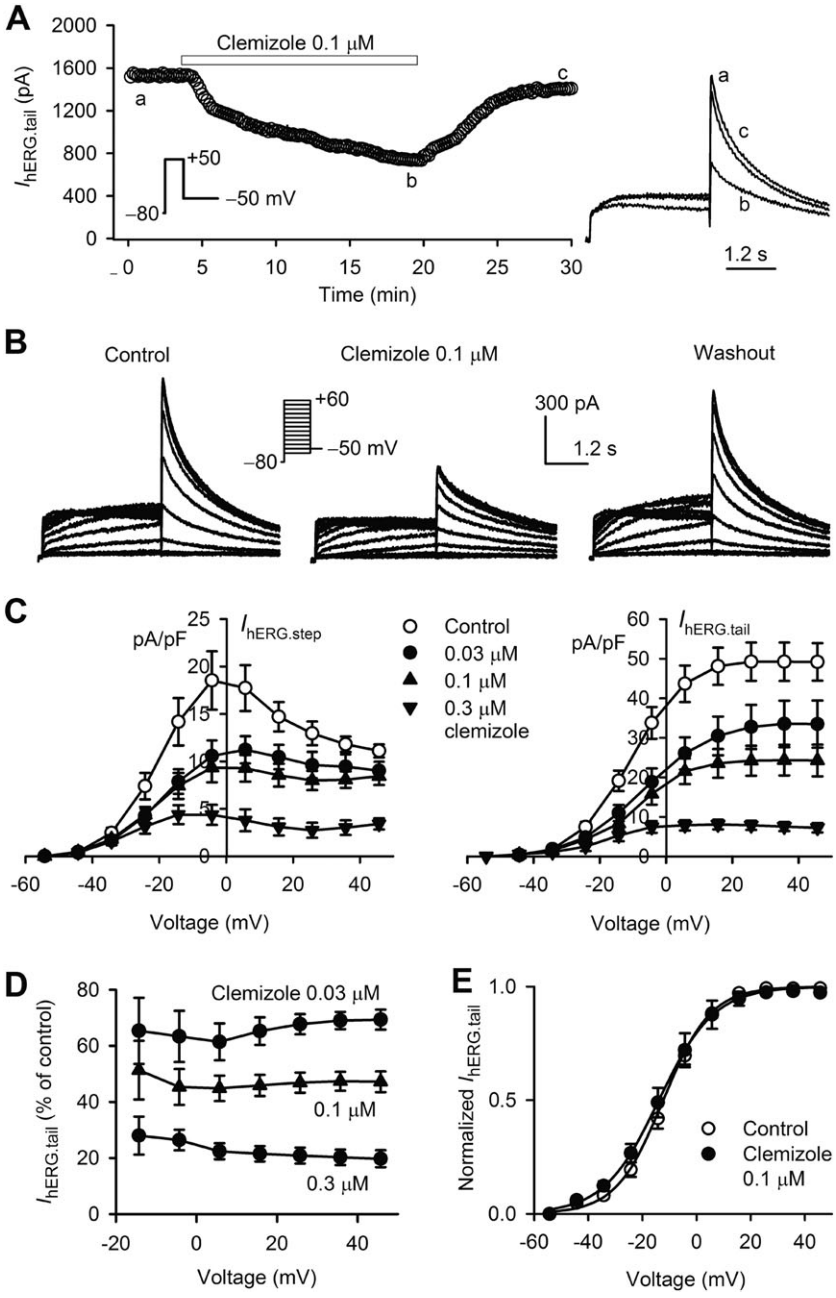

Figure 1

Inhibition of hERG channel current by clemizole. (A) Time-course of hERG tail current recorded in a HEK 293 cell stably expressing hERG channels during control (a), 0.1 μM clemizole (b) and washout (c). HERG current was elicited by the voltage protocol (inset): a 3 s voltage step to +50 mV from a holding potential of −80 mV, then back to −50 mV every 15 s. Current traces corresponding to a, b and c during the time course of $I_{hERG.tail}$ are shown on the right. (B) Voltage-dependent hERG current elicited by 3 s pulses to potentials between −60 and +60 mV from a holding potential of −80 mV, then back to −50 mV at 0.05 Hz (inset) in the absence and presence of 0.1 μM clemizole. (C) *I–V* relationships of $I_{hERG.tail}$ and $I_{hERG.step}$ in the absence and the presence of 0.03, 0.1 and 0.3 μM clemizole. Data shown are means ± SEM; $n = 8$. *$P < 0.05$, significantly different from control. (D) Fraction inhibitions of $I_{hERG.tail}$ at the testing potentials with 0.03, 0.1 and 0.3 μM clemizole. (E) *g–V* curve obtained by normalizing $I_{hERG.tail}$ at various voltages and fitting data to a Boltzmann equation before and after 0.1 μM clemizole ($n = 7$). The voltage range plotted for the voltage-dependent effects of clemizole on hERG current was post-corrected for liquid junction potential.

The IC_{50} values for clemizole were obtained by fitting the concentration–inhibition curves to a Hill equation (Figure 2C): $E = E_{max}/[1 + (IC_{50}/C)^b]$, where E is percentage inhibition of current at concentration C, E_{max} is the maximum inhibition, IC_{50} is the half maximal inhibitory concentration and b is the Hill coefficient. The efficacy of clemizole for inhibiting S636A, S631A, Y652A and F656V mutants were decreased by 10.7, 11.7, 20.1 and 41.5-fold respectively (relative

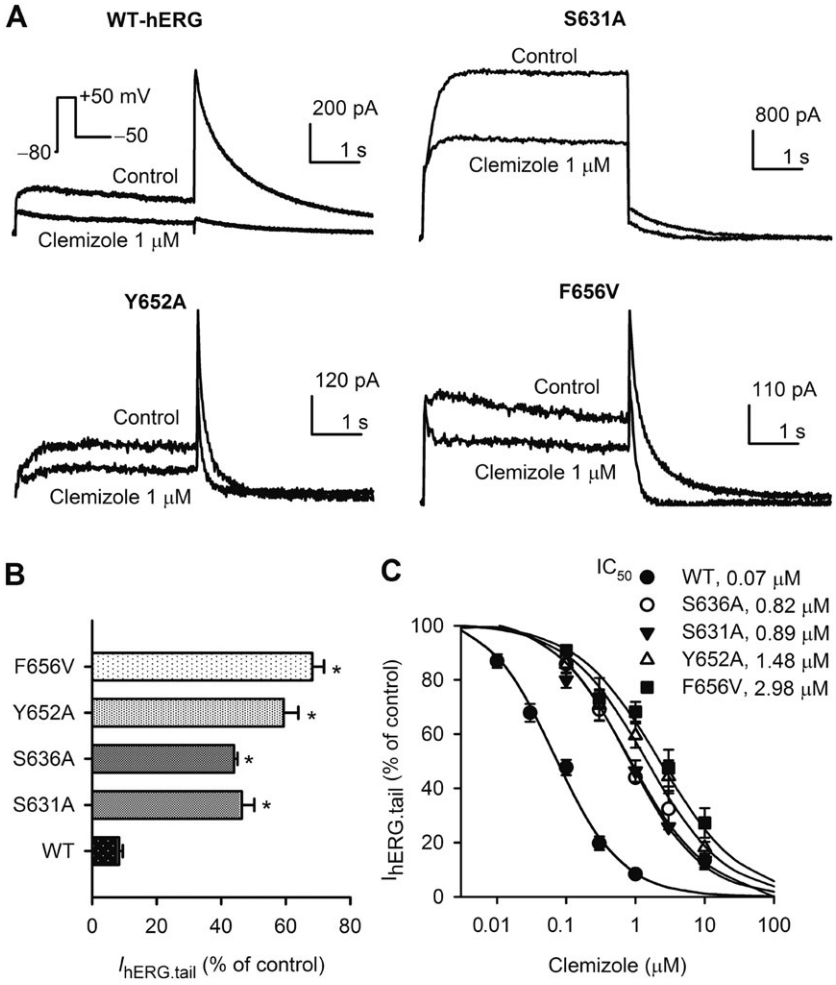

Figure 2

Molecular determinants of hERG channel block by clemizole. (A) Current traces recorded in HEK 293 cells expressing WT, S631A, Y652A and F656V hERG channels, respectively, before (control) and after 1 μM clemizole. Current was elicited by a 3 s voltage step to +50 mV from a holding potential of −80 mV, then back to −50 mV. (B) Inhibition of WT and mutant hERG tail currents by 1 μM clemizole. Data shown are means ± SEM; $n = 8$ for WT, $n = 7$ for mutants. *$P < 0.05$, significantly different from WT. (C) Concentration–inhibition relationships fitted to a Hill equation to obtain IC_{50} values of clemizole for inhibiting WT and various mutant hERG channels ($n = 7$ for each concentration).

to WT-hERG current). Therefore, the residues Ser^{631}, Ser^{636}, Tyr^{652} and Phe^{656} may be the major determinants of clemizole binding for blocking hERG channels.

The kinetics of inactivation play an important role in high-affinity drug binding to hERG channels (Smith *et al.*, 1996; Spector *et al.*, 1996; Guo *et al.*, 2006). The hERG channels were fully activated and inactivated by a depolarization voltage step to +50 mV, then a repolarization step to −100 mV for 10 ms to recover the channel from inactivation. The test steps were then clamped to different potentials to observe the time course of the voltage-dependent inactivation in the absence and presence of 0.1 μM clemizole (left panel of Figure 3A). The inactivation decay time constant was fitted to a mono-exponential equation. The voltage (post-corrected for the junctional potential) dependence of mean values of the time constant is illustrated in right panel of Figure 3A. Over most of the voltage range studied (−34.3 to +15.7 mV), clemizole (0.1 μM) significantly decreased the inactivation time ($n = 8$, $P < 0.05$), compared with control values, suggesting that clemizole accelerated the inactivation of the channel.

The effect of clemizole on steady-state inactivation (availability) of I_{hERG} was determined by a 20 ms voltage steps of −120 to +30 mV from a 4 s prepulse of +40 mV (left panel of Figure 3B) (Smith *et al.*, 1996; Tang *et al.*, 2008). The normalized I_{hERG} were fitted to the Boltzmann distribution (right panel of Figure 3B). The $V_{0.5}$ of I_{hERG} inactivation was negatively shifted by 0.1 μM clemizole from −61.1 ± 3.5 mV in control to −67.4 ± 3.2 mV in clemizole ($n = 7$, $P < 0.05$).

Recovery of hERG channels from inactivation was determined in the absence (control) and presence of 0.1 μM clemizole using a dual-pulse protocol (left panel of Figure 3C) as previously described (Spector *et al.*, 1996). The rising phase of the current was fitted to a mono-exponential function to obtain the recovery time constant. No difference was observed for the recovery time constant of hERG channels from

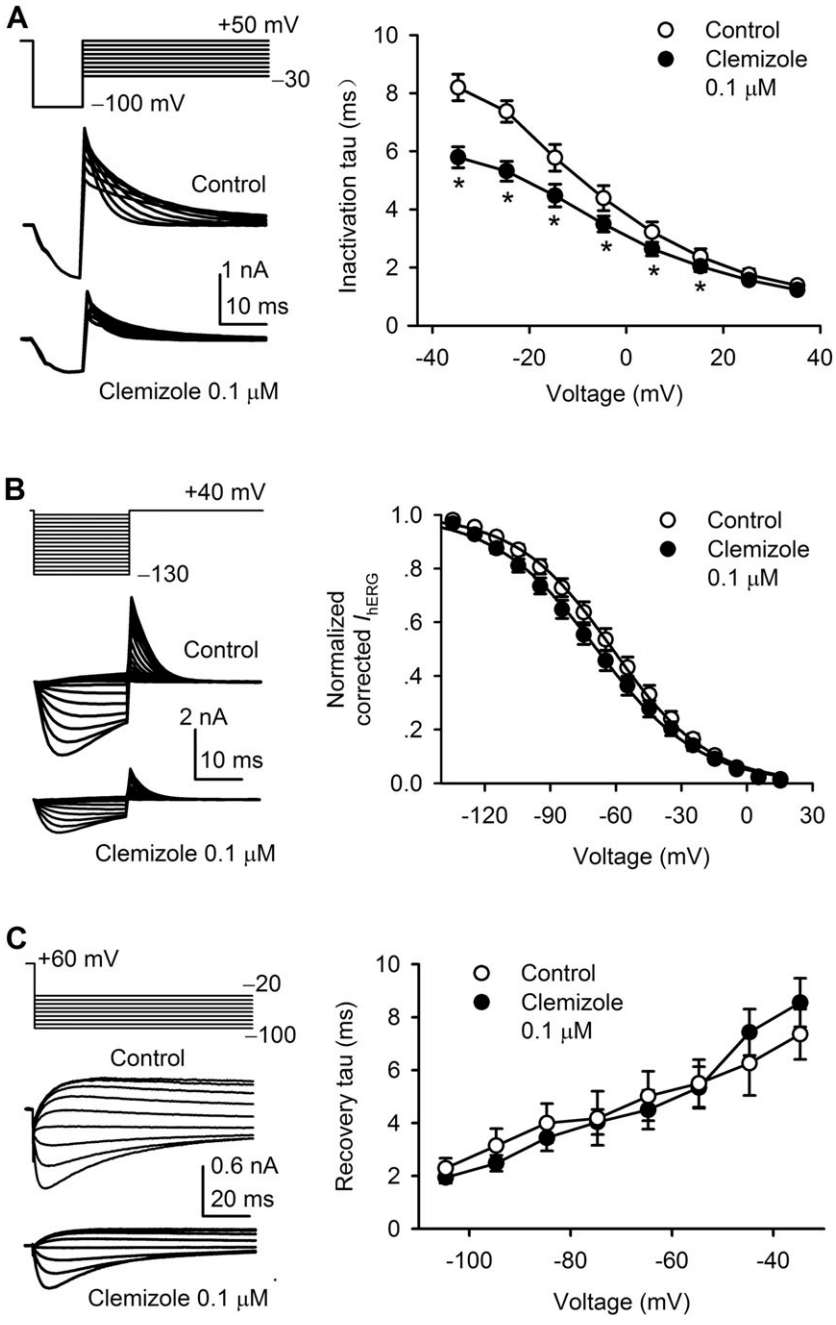

Figure 3

Effects of clemizole on hERG channel kinetics. (A) Left panel, the protocol and current traces before (control) and after 0.1 μM clemizole for the evaluation of inactivation time constant of hERG channels. Right panel, voltage dependent inactivation time constants (tau) in control and after application of 0.1 μM clemizole. Data shown are means ± SEM; $n = 8$. *$P < 0.05$, significantly different from control. (B) Left panel, the protocol and hERG current before (control) and after 0.1 μM clemizole used for determining steady-state inactivation of hERG channels. Right panel, steady-state inactivation curves of hERG current fitted to a Boltzmann equation. (C) Left panel, current traces recorded with the protocol were used to evaluate recovery time constant of hERG channels. The recovery phase of the current was fitted to a mono-exponential equation. Right panel, time constant (tau) of recovery from inactivation was not affected by 0.1 μM clemizole at all testing potential ($n = 6$, mean ± SEM). The voltage range plotted for the voltage-dependent kinetics of clemizole on hERG current was post-corrected for liquid junction potential.

inactivation, in the presence of 0.1 μM clemizole (right panel of Figure 3C, $n = 6$, $P > 0.05$ vs. control).

Time-dependent inhibition of I_{hERG} by clemizole was determined using a 11 s voltage step to 0 mV from −80 mV to open the channels. The development of I_{hERG} inhibition by 0.1 μM clemizole from the beginning of activation till the end of depolarization step would indicate whether clemizole is an open or closed channel blocker (Figure 4A).

The onset of open-channel blocking by 0.1 μM clemizole was assessed with the drug-sensitive current

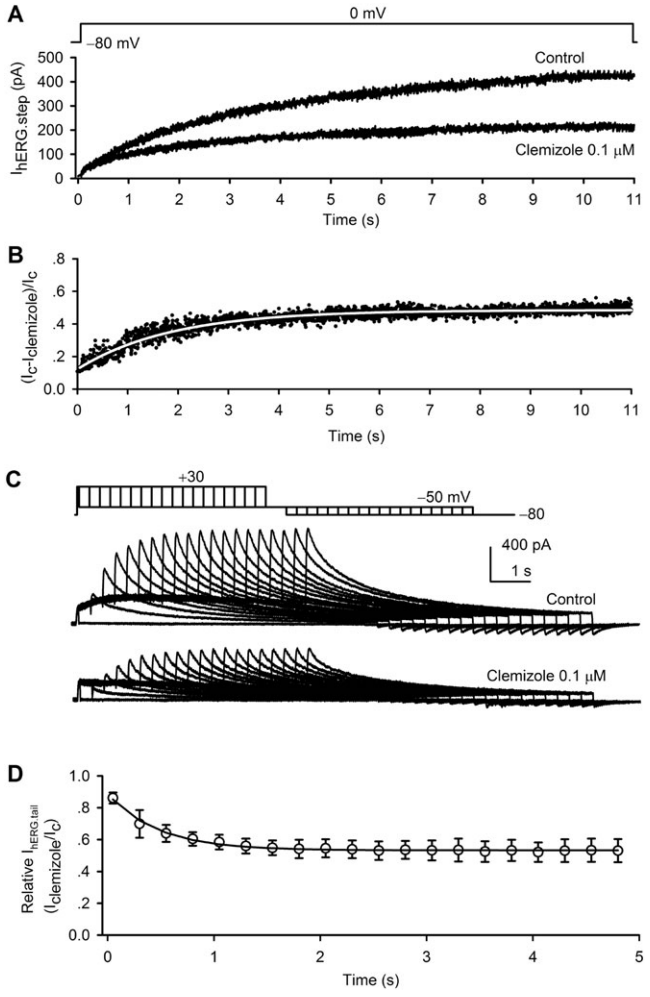

Figure 4

Development of hERG channel blocking by clemizole. (A) Voltage protocol and representative hERG current before and after 0.1 μM clemizole. (B) Drug-sensitive current expressed as a proportion of the current in the absence and the presence of 0.1 μM clemizole. Raw data (points) were fitted to a mono-exponential equation (solid white line). (C) Envelope of tails protocol and representative hERG current before (control) and after application of 0.1 μM clemizole. Cells were held at a holding potential of −80 mV and pulsed to depolarizing voltage (+30 mV) for variable durations from 50 to 4800 ms in 250 ms increments. $I_{hERG.tail}$ was recorded upon repolarization to −50 mV. (D) A plot of relative tail current with 0.1 μM clemizole versus the depolarizing duration. The time-dependent decay in relative tail current was fitted to a mono-exponential equation (mean ± SEM, n = 6).

formula: $[(I_C\text{-}I_D)/I_C]$ (Gao *et al.*, 2004), where I_C and I_D are the currents in the absence and presence of the drug respectively (Figure 4B). The initial current blocking of around 14% indicates a small fraction of closed (or tonic) channel blocking, and drug-sensitive current was fitted to a mono-exponential equation with the time constant of 471 ± 59.2 ms (n = 5), which suggests that the inhibition of hERG channels by clemizole involves blocking open channels. However, the potential contribution of tonic blocking and blockade of endogenous K^+ current by clemizole cannot be excluded.

The development of clemizole blocking of I_{hERG} was further evaluated with an envelope of tails test. Figure 4C shows the time course of the development of clemizole blocking effect on I_{hERG} assessed with the envelope of tails test (Zhang *et al.*, 2010). Cells were held at −80 mV, pulsed to a depolarizing potential (+30 mV) for variable durations ranging from 50 to 4950 ms and then repolarized to −50 mV. The envelope of tails tests were recorded in the same cell in the absence and presence of 0.1 μM clemizole.

The relative envelope tail current with 0.1 μM clemizole decayed in a pulse-duration-dependent manner (Figure 4D, n = 7). Tonic blockade of hERG current by clemizole was assessed by the initial value of the relative tail current activated by the envelope protocol. The current at 50 ms prepulse duration was inhibited by 15.1% compared with 47.0% at 4800 ms. So the tonic blocking fraction of hERG channels was about 32%, while open channel blocking was about 68% with 0.1 μM clemizole. This result indicates that clemizole has both closed- and open-channel blocking effects on hERG channels.

Effect of clemizole on I_{Ks}

The effect of clemizole on cardiac I_{Ks} was examined in HEK 293 cells stably expressing hKCNQ1/hKCNE1 plasmids. Figure 5A shows the voltage-dependent I_{Ks} traces recorded in a representative cell with 3 s voltage steps from −80 to +60 mV (10 mV increment), then to −50 mV from a holding potential of −80 mV before and after 3 μM clemizole. I_{Ks} was significantly decreased by clemizole and this effect was partly reversed by washout. Figure 5B displays the *I–V* relationships of I_{Ks} step current in cells treated with 1, 3 and 10 μM clemizole. The voltage range plotted for the voltage-dependent effect of clemizole on I_{Ks} was post-corrected for liquid junction potential. Significant suppression of the current was observed with 1 μM clemizole at +14.7 to +45.7 mV (n = 6, $P < 0.05$ vs. control), 3 and 10 μM clemizole at −4.3 to +45.7 mV (n = 6, $P < 0.05$ vs. control). The IC_{50} of clemizole for inhibiting human cardiac I_{Ks} step current (at +45.7 mV) shown in Figure 5C had a Hill coefficient of 0.9. No change was observed for current activation (normalized I_{Ks} tail current) with 3 μM clemizole ($V_{0.5}$: 1.5 ± 3.8 mV of control vs. 0.7 ± 4.3 mV, n = 8, $P > 0.05$)

Effect of clemizole on $hK_v1.5$ channel current

The effect of clemizole on $hK_v1.5$ channel current was determined in a stable HEK 293 cell line expressing the *KCN5A* gene. Figure 6A shows the voltage-dependent $hK_v1.5$ channel current recorded in a representative cell with the voltage protocol, as shown in the Figure inset, in the absence or presence of 3 μM clemizole. Clemizole significantly suppressed $hK_v1.5$ channel current, and the effect was reversed upon washout. Figure 6B displays the *I–V* relationships of $hK_v1.5$ channel current before (control) and after 3 and 10 μM clemizole. The voltage range plotted for the voltage-dependent effects of clemizole on this current was post-corrected for liquid junction potential. Significant reduction of $hK_v1.5$ channel current by clemizole, compared with control conditions, was observed at −4.3 to +45.7 mV (n = 6), and the inhibition was voltage-independent (Figure 6C). Figure 6D shows the current activation (normalized $hK_v1.5$ channel tail current) in the absence and presence of 3 μM clemizole and fitted to

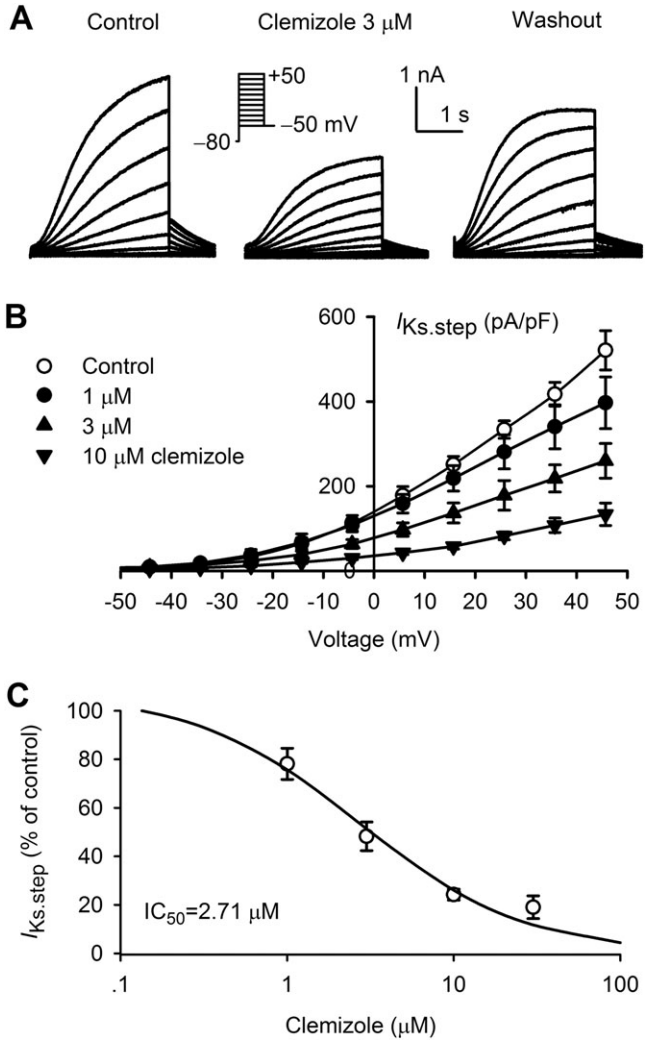

Figure 5

Inhibition of human cardiac I_{Ks} by clemizole. (A) Voltage-dependent I_{Ks} recorded in a representative HEK 293 cell with the voltage protocol as shown in the inset in the absence and the presence of 3 μM clemizole. (B) *I–V* relationships of I_{Ks} in the absence and the presence of 1, 3 and 10 μM clemizole (mean ± SEM, $n = 6$). The voltage range plotted for the voltage-dependent effect of clemizole on I_{Ks} was post-corrected for liquid junction potential. (C) Concentration–inhibition relationships of clemizole for inhibiting I_{Ks}. Data were fitted to a Hill equation (mean ± SEM, $n = 7$ for each concentration).

the Boltzmann function. The $V_{0.5}$ of $hK_v1.5$ channel activation was not altered by clemizole ($V_{0.5}$: 1.1 ± 0.8 mV of control vs. −1.3 ± 0.6 mV, $n = 7$, $P > 0.05$). The IC_{50} of clemizole for inhibiting $hK_v1.5$ channel current (at +45.7 mV) shown in Figure 6E had a Hill co-efficient of 1.1.

Effect of clemizole on ventricular action potentials

Whether the inhibition of I_{hERG} and I_{Ks} by clemizole leads to a prolongation of ventricular APD was determined in guinea pig ventricular myocytes (37°C). Figure 7A illustrates the ventricular action potentials recorded (2 Hz) in a representative myocyte before (control) and after application of 0.1, 0.3, 1 and 3 μM clemizole. APD was progressively prolonged with increasing concentrations of clemizole. The effect was partially recovered on drug washout.

Figure 7B shows the individual and mean values of APD at 50 and 90% repolarization (APD_{50} and APD_{90}) in ventricular myocytes of guinea pig hearts. Clemizole (0.1–3 μM) prolonged both APD_{50} and APD_{90} ($n = 5$–10), compared with control. Changes in resting membrane potential and action potential amplitude were not observed over this concentration range of clemizole (data not shown), suggesting that clemizole did not significantly inhibit sodium channels or the inward rectifier K^+ current (I_{K1}).

Clemizole prolongs ECG QTc interval in ex vivo *guinea pig hearts*

It is generally believed that the suppression of I_{hERG} and/or I_{Ks} and ventricular APD prolongation implies a potential for cardiac toxicity, that is, increasing the QT interval of the ECG (Yang *et al.,* 2004; Hauser *et al.,* 2005; Takahara *et al.,* 2006). To investigate whether clemizole has the potential of increasing QT interval, we determined the effect of clemizole on the QTc interval of ECG and other parameters in guinea pig isolated and perfused hearts. Figure 8A shows the ECG traces and LVSP and the pressure velocity during heart contraction/relaxation (dP/dT) in a representative experiment in a heart before and after perfusion with 1 μM clemizole for 10 min. Clemizole decreased the heart rate and prolonged QT interval. The average values of heart rate and QTc interval are shown in Figure 8B. Heart rate was decreased by 0.3 and 1 μM clemizole, while QTc interval was increased with these concentrations. However, the width of the QRS complex and the cardiac contractile parameters LVSP and +dP/dT were not changed by any concentration of clemizole (Figure 8C).

Discussion

Clemizole is a histamine H_1-receptor antagonist drug, first developed in the 1950s (Zierz and Greither, 1952; Naranjo and De Naranjo, 1958). Early studies showed that clemizole has a high antihistamine specificity with low toxicity in acute and chronic observations in animal experiments (Finkelstein *et al.,* 1960). Clemizole is clinically used for allergic rhinitis (Jacques and Fuchs, 1960) and pruritus of dermatoses (Wansker, 1962; Osment and Broyles, 1963). Clemizole-penicillin is widely employed for antiluetic therapy (Kleinhans, 1971; Kirwald and Montag, 1999; Heise, 2004). In addition, an earlier study in dogs demonstrated that clemizole effectively converted atrial flutter induced by circus movement into sinus rhythm by increasing the atrial refractory period without significant reduction in conduction velocity (Mendez *et al.,* 1969).

A previous study with high-throughput screening identified 18 compounds that inhibit binding of the viral protein NS4B to RNA and found that clemizole inhibited HCV RNA replication in host cell culture with little toxicity, suggesting that clemizole is a promising candidate for the pharmaceutical development of anti-HCV compounds (Einav *et al.,* 2008). The antiviral effect of clemizole was found to be

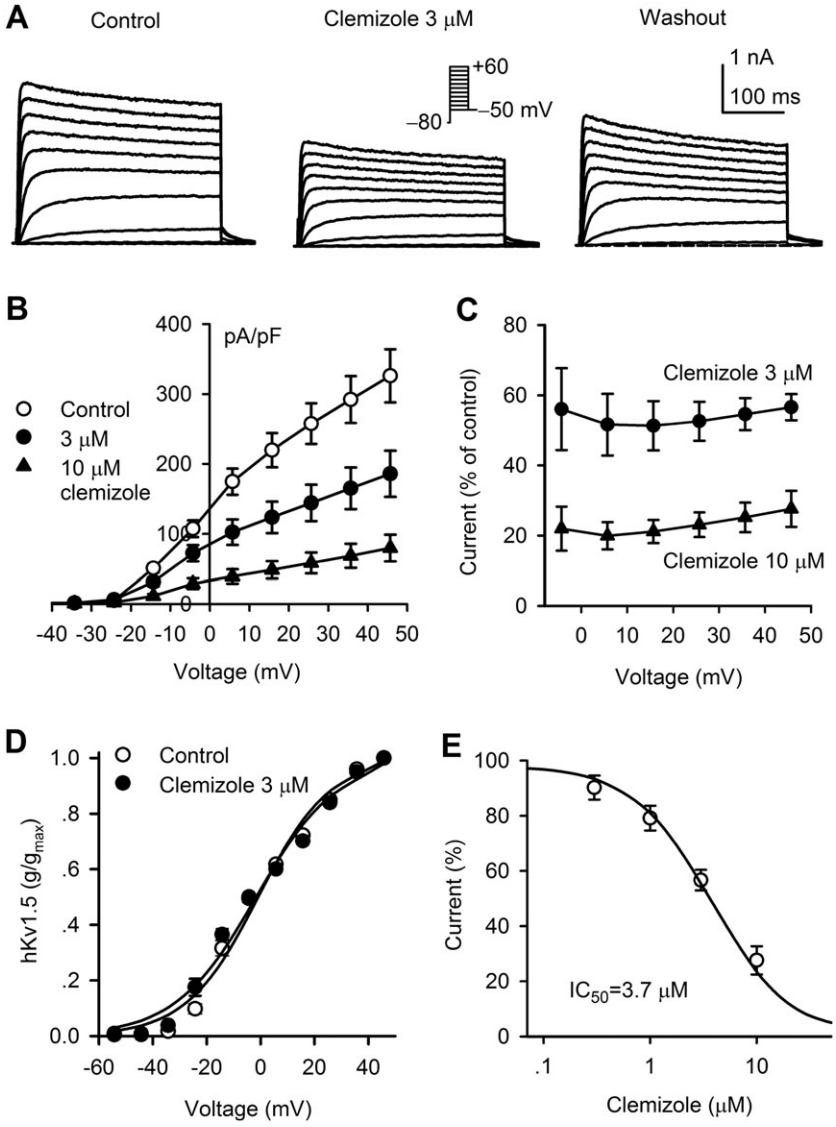

Figure 6

Effect of clemizole on hK$_v$1.5 channel current. (A) Voltage-dependent hK$_v$1.5 channel current traces recorded in a representative HEK 293 cell using the protocol as shown in the inset in the absence and the presence of 3 μM clemizole. (B) Current–voltage relationships of hK$_v$1.5 channel current in the absence and the presence of 3 and 10 μM clemizole (mean ± SEM, $n = 6$). (C) Fraction of hK$_v$1.5 channel current inhibition by 3 and 10 μM clemizole at voltages ranging from −14.3 to +34.7 mV. (D) Activation conductance curves before and after 3 μM clemizole ($n = 7$). The curves were obtained by normalizing hK$_v$1.5 channel tail current at various voltages to the maximal values and fitting the data to a Boltzmann distribution. (E) Concentration–inhibition relationships of clemizole for inhibiting hK$_v$1.5 channel current. Data were fitted to a Hill equation (mean ± SEM, $n = 7$ for each concentration). The voltage range plotted for the voltage-dependent parameters of clemizole on hK$_v$1.5 channel current was post-corrected for liquid junction potential.

remarkably synergized by combination with either interferon or ribavirin and the HCV protease inhibitors VX950 and SCH503034 (Einav *et al.*, 2010). Although clemizole has a short plasma half-life with rapid biotransformation, the predominant glucuronide and dealkylated metabolites in human still retain synergistic anti-HCV activity (Nishimura *et al.*, 2013). A phase 1 clinical trial (NCT00945880) of clemizole has been carried out to evaluate safety and tolerability to treat hepatitis C (https://www.clinicaltrials.gov/ct2/show/NCT00945880). Although there is no published clinical trial data available, clemizole might have the potential for long-term clinical use to treat patients with hepatitis C in the future.

In this study, we have demonstrated that clemizole inhibited cardiac hERG (encoding for cardiac I_{Kr}) and hKCNQ1/hKCNE1 (encoding for cardiac I_{Ks}) channels, and also hKv1.5 (encoding for cardiac I_{Kur}) channels, prolonged APD in guinea pig ventricular myocytes and QTc interval in *ex vivo* guinea pig hearts. These effects may account for its antiarrhythmic effect of converting atrial flutter into sinus rhythm observed in anaesthetized dogs (Mendez *et al.*, 1969). However, these effects may also imply that clemizole

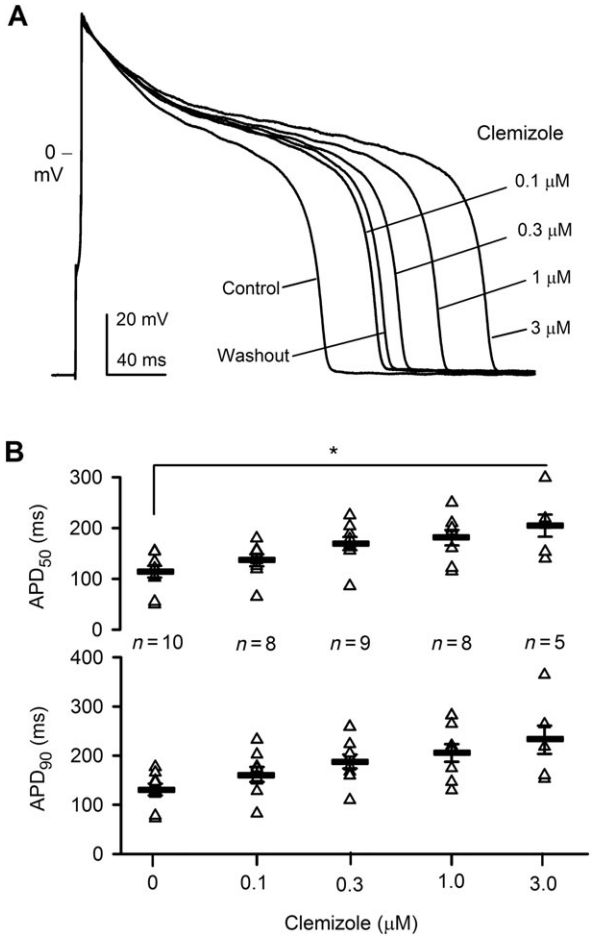

Figure 7

Effects of clemizole on action potentials in isolated ventricular myocytes from guinea pig hearts. (A). Action potentials recorded (2 Hz) in current clamp mode in a representative myocyte in the absence (control) and presence of 0.1, 0.3, 1 and 3 μM clemizole and washout. (B). Individual (triangle symbols) and mean (thick horizontal lines) values of APD_{50} and APD_{90} in the absence and presence of 0.1, 0.3, 1 and 3 μM clemizole; mean ± SEM, n = 5–10. *$P < 0.05$, significantly different from control.

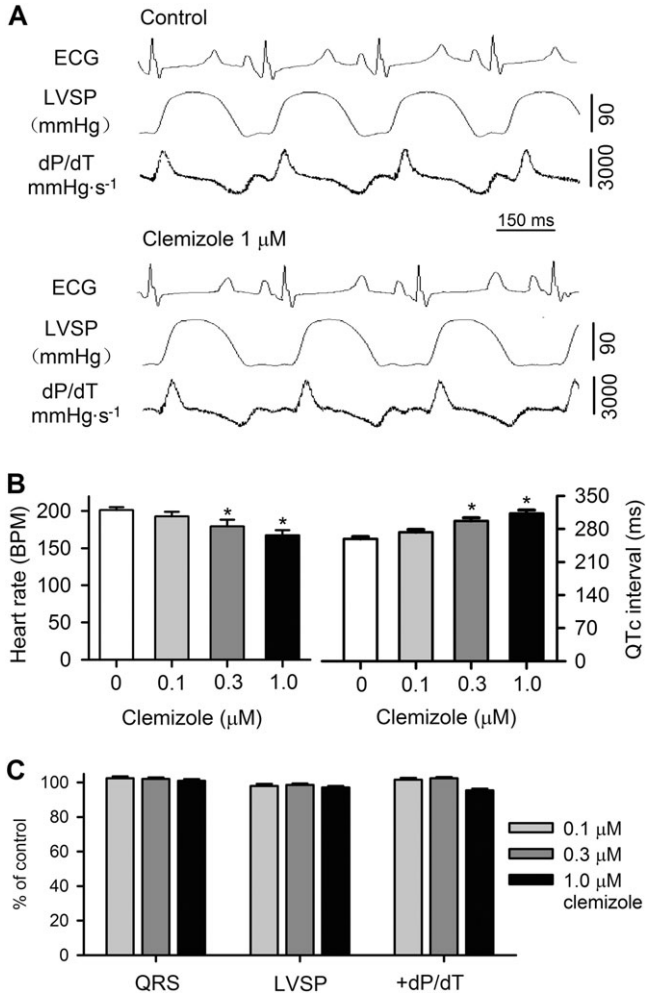

Figure 8

Effects of clemizole on ECG and contractile function in guinea pig isolated perfused hearts. (A) Representative ECG and heart contractile parameters (LVSP and dP/dT) recorded in a heart before (control) after 1 μM clemizole application. (B) Heart rates (BPM) and QTc interval (ms) in hearts before and after treatment with 0.1, 0.3 and 1 μM clemizole. Data shown are means ± SEM (n = 7). *$P < 0.05$, significantly different from control). (C) Changes in QRS complex, LVSP and +dP/dT after 0.1, 0.3 and 1 μM clemizole. Data shown are means ± SEM; n = 7, $P > 0.05$, significantly different from vehicle).

has cardiac toxicity and has the potential to cause long QT syndrome or Torsade de pointes (TdPs).

It is well documented that drugs that prolong QTc interval, in general, by blocking I_{Kr} or hERG channels although patients with drug-induced TdPs may have additional cardiac risk factors (Sanguinetti and Tristani-Firouzi, 2006; Gupta *et al.*, 2007; Isbister and Page, 2013). We found that clemizole decreased the current carried by hERG channels stably expressed in HEK 293 cells, in a concentration-dependent manner with an IC_{50} of 70 nM. The inhibition was related to blocking closed and open channels and accelerating hERG channel inactivation without affecting steady-state availability or recovery. The blocking properties of clemizole for hERG channels are similar to those observed with the selective oestrogen receptor modulator, raloxifene (Liu *et al.*, 2010).

The blocking effect of clemizole was reduced by >10-fold in the mutant hERG channels, S631A and S636A, which exhibit deficient channel inactivation, suggesting that the inactivation is required for high-affinity blockade of the channel by clemizole, which is similar to the selective-serotonin re-uptake inhibitor fluvoxamine (Milnes *et al.*, 2003), cocaine (Guo *et al.*, 2006) and the calmodulin inhibitor W-7 (Zhang *et al.*, 2010). The hERG mutants Y652A and F656V also showed markedly reduced (20- to 40-fold) inhibition of hERG current by clemizole. This may suggest that the binding of clemizole is involved at Tyr^{652} and Phe^{656}, and that the hydrophobicity of the side chain residues of Tyr^{652} and Phe^{656} is related to the channel sensitivity to clemizole. Therefore, Y652 and F656 are likely to be important sites for the binding of clemizole to hERG channels, as has been already observed for cisapride, terfenadine, MK-499 (Fernandez *et al.*, 2004) and fluvoxamine (Milnes *et al.*, 2003). Although these results indicate that these four residues S631, S636,

Y652 and F656 are major molecular determinants of clemizole blockade of the channel, the possibility of binding to other amino acids cannot be excluded. A whole new series of experiments would be required to carry out an alanine scan of the whole S6 segment (Kamiya *et al.,* 2006) to assess the binding of clemizole to other amino acids.

The drug-induced negative chronotropic effect is usally related to the inhibition of Ca^{2+} current (I_{Ca}) and/or pacemaker current (i.e. funny current I_f, encoded by HCN2/HCN4 channels, and the hyperpolarization-activated cyclic nucleotide-gated ion channels). In this study, we found that clemizole significantly reduced heart rate in guinea pig hearts *ex vivo*. However, the effect seemed to be unrelated to the mechanisms described above, because clemizole increased guinea pig ventricular APD, prolonged QTc interval without reducing the cardiac contractile function parameters LVSP and ±dP/dT and did not show any inhibition of I_f channels in HEK 293 cells expressing HCN2 or HCN4 channels with 1 μM clemizole (Figure S1). The likely cause of the heart rate reduction by clemizole is the I_{Kr}/hERG channel blockade. This is supported by an earlier report, in which E4031 blocked I_{Kr} and decreased sinus rhythm in adult mouse sinoatrial node cells (Clark *et al.,* 2004).

Drug effects on I_{Ks} and QT interval are not well recognized. However, norfluoxetine (a selective serotonin reuptake inhibitor) prolonged QT interval in a patient with KCNQ1 mutation, and therefore, I_{Ks} blockade may also be involved in drug-induced long QT syndrome when repolarization reserve is reduced (Veerman *et al.,* 2013). In the present study, we found that clemizole decreased hKCNQ1/hKCNE1 channels expressed in HEK 293 cells. The IC_{50} of clemizole for inhibiting I_{Ks} was 2.7 μM, which may also contribute to the prolongation of APD and QT interval in guinea pig ventricular myocytes and guinea pig isolated hearts. Clemizole decreased $hK_v1.5$ channel current expressed in HEK 293 cells with an IC_{50} of 3.7 μM, suggesting that clemizole may be an non-selective channel blocker. In addition to blockade of cardiac K^+ currents, a recent study demonstrated that clemizole might be a potential TRPC5 channel blocker (Richter *et al.,* 2014).

The TRPC channels are present in many different types of cells and tissues in mammals, including humans. In addition to the regulation of various cellular physiological functions, they mediate a range of patho-physiological processes, for example, cardiac hypertrophy and fibrosis, vascular disorders, cancer, inflammation and neurodegenerative disorders and thus are considered to be pharmacological targets (Pena and Ordaz, 2008; Kaneko and Szallasi, 2013; Nilius, 2013). Although a great effort has been made to identify selective TRPC channel blockers, no selective antagonists are available for clinical trials. The general TRPC channel blocker, SKF-96365, also inhibited the voltage-gated sodium current I_{Na} (Chen *et al.,* 2015), the voltage-gated calcium current $I_{Ca.L}$ (Franzius *et al.,* 1994) and $I_{Ca.T}$ (Singh *et al.,* 2010), several cardiac potassium currents, including I_{hERG}, I_{Ks}, $K_{ir}2.1/I_{K1}$ and $K_v4.3/I_{to}$) and induced the long QT syndrome (Liu *et al.,* 2016). The report that clemizole might be a potent blocker of TRPC5 channels (Richter *et al.,* 2014) is attractive and interesting. Nonetheless, the present study demonstrated that clemizole decreased several cardiac K^+ channels, especially hERG channels, and caused a prolongation of QT interval. While Pyr3 is a selective antagonist of TRPC3 channels (Kiyonaka *et al.,* 2009), it is still experimental (Munakata *et al.,* 2013). Therefore, further effort is needed to develop more selective TRPC inhibitors for novel therapeutic use.

Although clemizole has been developed for many years, it is not administered systemically in clinical use, as it is used topically for allergic rhinitis (Jacques and Fuchs, 1960), allergic reactions and dermal diseases (Finkelstein *et al.,* 1960; Jacques and Fuchs, 1960; Wansker, 1962). Therefore, cardiac toxicity (QTc prolongation/TdP with clemizole) has not been reported. The more recent studies on clemizole have uncovered its therapeutic potential for treating HCV infection (Einav *et al.,* 2008) and the rare but severe genetic disease, Dravet syndrome (Baraban *et al.,* 2013) and its blocking effect on TRPC5 ion channels (Richter *et al.,* 2014). This study demonstrated that clemizole blocked I_{hERG} with a IC_{50} of 70 nM, which is 10-fold lower than the plasma level (767 nM) found in patients in the clinical trial for treating hepatitis C (https://www.clinicaltrials.gov/ct2/show/NCT00945880; Nishimura *et al.,* 2013) and the IC_{50} (1 μM) for blocking TRPC5 channels (Richter *et al.,* 2014). The high sensitivity of clemizole for blocking I_{hERG} and inhibiting I_{Ks} (IC_{50} of 2.7 μM) implies that this compound has potential to cause QTc prolongation and /or TdP. Therefore, its potential for cardiac toxicity must be considered when it is used long-term to treat HCV infections. Similarly, interpretation of experimental results obtained in native cardiac cells using clemizole as a blocker of TRPC channels, must allow for its effects on hERG and other K^+ channels.

Acknowledgements

This work was supported in part by a Key Cardiovascular Laboratory Fund (3502Z20150050) from Department of Xiamen Science and Technology, Xiamen, China. The authors thank Ms Hai-Ying Sun for the excellent technical support.

Author contributions

L.J.J., W.Y.W., G.S.X., S.Z., G.R.L. and Y.W. conceived and designed the experiments; L.J.J., W.Y.W. and G.L. performed the experiments; L.J.J. and G.R.L. analysed the data; L.J.J. and G.R.L. wrote the paper; and L.J.J., W.Y.W., G.L., G.S.X., S.Z., G.R.L. and Y.W. approved the submission.

Conflict of interest

The authors declare no conflicts of interest.

Declaration of transparency and scientific rigour

This Declaration acknowledges that this paper adheres to the principles for transparent reporting and scientific rigour of preclinical research recommended by funding agencies, publishers and other organisations engaged with supporting research.

References

Alexander SPH, Catterall WA, Kelly E, Marrion N, Peters JA, Benson HE *et al.* (2015). The concise guide to PHARMACOLOGY 2015/16: Voltage-gated ion channels. Br J Pharmacol 172: 5904–5941.

Baraban SC, Dinday MT, Hortopan GA (2013). Drug screening in SCN1a zebrafish mutant identifies clemizole as a potential Dravet syndrome treatment. Nat Commun 4: 2410.

Chen KH, Liu H, Yang L, Jin MW, Li GR (2015). SKF-96365 strongly inhibits voltage-gated sodium current in rat ventricular myocytes. Pflugers Arch 467: 1227–1236.

Clark RB, Mangoni ME, Lueger A, Couette B, Nargeot J, Giles WR (2004). A rapidly activating delayed rectifier K^+ current regulates pacemaker activity in adult mouse sinoatrial node cells. Am J Physiol Heart Circ Physiol 286: H1757–H1766.

Curtis MJ, Bond RA, Spina D, Ahluwalia A, Alexander SP, Giembycz MA *et al.* (2015). Experimental design and analysis and their reporting: new guidance for publication in BJP. Br J Pharmacol 172: 3461–3471.

Einav S, Gerber D, Bryson PD, Sklan EH, Elazar M, Maerkl SJ *et al.* (2008). Discovery of a hepatitis C target and its pharmacological inhibitors by microfluidic affinity analysis. Nat Biotechnol 26: 1019–1027.

Einav S, Sobol HD, Gehrig E, Glenn JS (2010). The hepatitis C virus (HCV) NS4B RNA binding inhibitor clemizole is highly synergistic with HCV protease inhibitors. J Infect Dis 202: 65–74.

Fernandez D, Ghanta A, Kauffman GW, Sanguinetti MC (2004). Physicochemical features of the HERG channel drug binding site. J Biol Chem 279: 10120–10127.

Finkelstein M, Kromer CM, Sweeney SA, Delahunt CS (1960). Some aspects of the pharmacology of clemizole hydrochloride. J Am Pharm Assoc Am Pharm Assoc 49: 18–22.

Franzius D, Hoth M, Penner R (1994). Non-specific effects of calcium entry antagonists in mast cells. Pflugers Arch 428: 433–438.

Gao Z, Lau CP, Chiu SW, Li GR (2004). Inhibition of ultra-rapid delayed rectifier K^+ current by verapamil in human atrial myocytes. J Mol Cell Cardiol 36: 257–263.

Guo J, Gang H, Zhang S (2006). Molecular determinants of cocaine block of human ether-a-go-go-related gene potassium channels. J Pharmacol Exp Ther 317: 865–874.

Gupta A, Lawrence AT, Krishnan K, Kavinsky CJ, Trohman RG (2007). Current concepts in the mechanisms and management of drug-induced QT prolongation and torsade de pointes. Am Heart J 153: 891–899.

Hauser DS, Stade M, Schmidt A, Hanauer G (2005). Cardiovascular parameters in anaesthetized guinea pigs: a safety pharmacology screening model. J Pharmacol Toxicol Methods 52: 106–114.

Heise H (2004). Current syphilis therapies and serological control. Commentary on the article by M. Hartmann in Hautarzt, Volume 2 (2004). Hautarzt 55: 1087–1089.

Isbister GK, Page CB (2013). Drug induced QT prolongation: the measurement and assessment of the QT interval in clinical practice. Br J Clin Pharmacol 76: 48–57.

Jacques AA, Fuchs VH (1960). Clinical evaluation of clemizole in allergic rhinitis. Int Rec Med 173: 88–91.

Kamiya K, Niwa R, Mitcheson JS, Sanguinetti MC (2006). Molecular determinants of HERG channel block. Mol Pharmacol 69: 1709–1716.

Kaneko Y, Szallasi A (2013). TRP channels as therapeutic targets. Curr Top Med Chem 13: 241–243.

Kilkenny C, Browne W, Cuthill IC, Emerson M, Altman DG (2010). Animal research: Reporting *in vivo* experiments: the ARRIVE guidelines. Br J Pharmacol 160: 1577–1579.

Kirwald H, Montag A (1999). Stage 3 syphilis of the mouth cavity. Laryngorhinootologie 78: 254–258.

Kiyonaka S, Kato K, Nishida M, Mio K, Numaga T, Sawaguchi Y*et al.* (2009). Selective and direct inhibition of TRPC3 channels underlies biological activities of a pyrazole compound. Proc Natl Acad Sci U S A 106: 5400–5405.

Kleinhans D (1971). Blood level studies on the depot effect of clemizole-penicillin G in antiluetic therapy. Z Haut Geschlechtskr 46: 359–365.

Li GR, Lau CP, Shrier A (2002). Heterogeneity of sodium current in atrial vs epicardial ventricular myocytes of adult guinea pig hearts. J Mol Cell Cardiol 34: 1185–1194.

Liu H, Sun HY, Lau CP, Li GR (2007). Regulation of voltage-gated cardiac sodium current by epidermal growth factor receptor kinase in guinea pig ventricular myocytes. J Mol Cell Cardiol 42: 760–768.

Liu H, Yang L, Jin MW, Sun HY, Huang Y, Li GR (2010). The selective estrogen receptor modulator raloxifene inhibits cardiac delayed rectifier potassium currents and voltage-gated sodium current without QTc interval prolongation. Pharmacol Res 62: 384–390.

Liu H, Yang L, Chen KH, Sun HY, Jin MW, Xiao GS *et al.* (2016). SKF-96365 blocks human ether-à-go-gorelated gene potassium channels stably expressed in HEK 293 cells. Pharmacol Res 104: 61–69.

McGrath JC, Lilley E (2015). Implementing guidelines on reporting research using animals (ARRIVE etc.): new requirements for publication in BJP. Br J Pharmacol 172: 3189–3193.

Mendez R, Kabela E, Pastelin G, Martinez-Lopez M, Sanchez-Perez S (1969). Antiarrhythmic actions of clemizole as pharmacologic evidence for a circus movement mechanism in atrial flutter. Naunyn Schmiedebergs Arch Exp Pathol Pharmakol 262: 325–336.

Milnes JT, Crociani O, Arcangeli A, Hancox JC, Witchel HJ (2003). Blockade of HERG potassium currents by fluvoxamine: incomplete attenuation by S6 mutations at F656 or Y652. Br J Pharmacol 139: 887–898.

Morissette P, Regan HK, Fitzgerald K, Bernasconi S, Gerenser P, Travis J *et al.* (2015). QT interval correction assessment in the anesthetized guinea pig. J Pharmacol Toxicol Methods 75: 52–61.

Munakata M, Shirakawa H, Nagayasu K, Miyanohara J, Miyake T, Nakagawa T*et al.* (2013). Transient receptor potential canonical 3 inhibitor Pyr3 improves outcomes and attenuates astrogliosis after intracerebral hemorrhage in mice. Stroke 44: 1981–1987.

Naranjo P, De Naranjo EB (1958). Local anesthetic activity of some antihistamines and its relationship with the antihistaminic and anticholinergic activities. Arch Int Pharmacodyn Ther 113: 313–335.

Nilius B (2013). Transient receptor potential TRP channels as therapeutic drug targets: next round! Curr Top Med Chem 13: 244–246.

Nishimura T, Hu Y, Wu M, Pham E, Suemizu H, Elazar M *et al.* (2013). Using chimeric mice with humanized livers to predict human drug metabolism and a drug–drug interaction. J Pharmacol Exp Ther 344: 388–396.

Osment LS, Broyles JA (1963). Pruritus of dermatoses treated adjunctively with oral clemizole hydrochloride. Clin Med (Northfield) 70: 1637–1640.

Pena F, Ordaz B (2008). Non-selective cation channel blockers: potential use in nervous system basic research and therapeutics. Mini Rev Med Chem 8: 812–819.

Richter JM, Schaefer M, Hill K (2014). Clemizole hydrochloride is a novel and potent inhibitor of transient receptor potential channel TRPC5. Mol Pharmacol 86: 514–521.

Sanguinetti MC, Tristani-Firouzi M (2006). hERG potassium channels and cardiac arrhythmia. Nature 440: 463–469.

Singh A, Hildebrand ME, Garcia E, Snutch TP (2010). The transient receptor potential channel antagonist SKF96365 is a potent blocker of low-voltage-activated T-type calcium channels. Br J Pharmacol 160: 1464–1475.

Smith PL, Baukrowitz T, Yellen G (1996). The inward rectification mechanism of the HERG cardiac potassium channel. Nature 379: 833–836.

Southan C, Sharman JL, Benson HE, Faccenda E, Pawson AJ, Alexander SPH *et al.* (2016). The IUPHAR/BPS guide to PHARMACOLOGY in 2016: towards curated quantitative interactions between 1300 protein targets and 6000 ligands. Nucl Acids Res 44 (Database Issue): D1054–D1068.

Spector PS, Curran ME, Zou A, Keating MT, Sanguinetti MC (1996). Fast inactivation causes rectification of the IKr channel. J Gen Physiol 107: 611–619.

Su Z, Martin R, Cox BF, Gintant G (2004). Mesoridazine: an open-channel blocker of human ether-a-go-go-related gene K+ channel. J Mol Cell Cardiol 36: 151–160.

Takahara A, Sugiyama A, Hashimoto K (2005). Reduction of repolarization reserve by halothane anaesthesia sensitizes the guinea-pig heart for drug-induced QT interval prolongation. Br J Pharmacol 146: 561–567.

Takahara A, Sugiyama A, Hashimoto K (2006). Characterization of the halothane-anesthetized guinea-pig heart as a model to detect the K+ channel blocker-induced QT-interval prolongation. Biol Pharm Bull 29: 827–829.

Tang Q, Li ZQ, Li W, Guo J, Sun HY, Zhang XH *et al.* (2008). The 5-HT2 antagonist ketanserin is an open channel blocker of human cardiac ether-a-go-go-related gene (hERG) potassium channels. Br J Pharmacol 155: 365–373.

Van de Water A, Verheyen J, Xhonneux R, Reneman RS (1989). An improved method to correct the QT interval of the electrocardiogram for changes in heart rate. J Pharmacol Methods 22: 207–217.

Vandenberg JI, Perry MD, Perrin MJ, Mann SA, Ke Y, Hill AP (2012). hERG K(+) channels: structure, function, and clinical significance. Physiol Rev 92: 1393–1478.

Veerman CC, Verkerk AO, Blom MT, Klemens CA, Langendijk PN, van Ginneken AC *et al.* (2013). Slow delayed rectifier potassium current blockade contributes importantly to drug-induced long QT syndrome. Circ Arrhythm Electrophysiol 6: 1002–1009.

Wansker BA (1962). Clemizole hydrochloride: a clinical evaluation of its antipruritic effect. Skin (Los Angeles) 1: 157–159.

Yang Z, Shi G, Li C, Wang H, Liu K, Liu Y (2004). Electrophysiologic effects of nicorandil on the guinea pig long QT1 syndrome model. J Cardiovasc Electrophysiol 15: 815–820.

Zhang S, Zhou Z, Gong Q, Makielski JC, January CT (1999). Mechanism of block and identification of the verapamil binding domain to HERG potassium channels. Circ Res 84: 989–998.

Zhang DY, Wang Y, Lau CP, Tse HF, Li GR (2008). Both EGFR kinase and Src-related tyrosine kinases regulate human ether-a-go-go-related gene potassium channels. Cell Signal 20: 1815–1821.

Zhang XH, Jin MW, Sun HY, Zhang S, Li GR (2010). The calmodulin inhibitor N-(6-aminohexyl)-5-chloro-1-naphthalene sulphonamide directly blocks human ether a-go-go-related gene potassium channels stably expressed in human embryonic kidney 293 cells. Br J Pharmacol 161: 872–884.

Zierz P, Greither H (1952). Clinical evaluation of allercur, a new antihistaminic. Arztl Wochensch 7: 704–707.

Supporting Information

Additional Supporting Information may be found in the online version of this article at the publisher's web-site:

http://doi.org/10.1111/bph.13679

Figure S1 Effects of clemizole on HCN2 and HCN4 channels, stably expressed in HEK 293 cells. A. HCN2 channel current traces recorded with the voltage protocol shown above the traces in the absence (control) and presence of 1 μM clemizole (8 min). Clemizole had no effect on HCN2, and similar results were obtained in additional 3 sets of cells. B. HCN4 channel current traces recorded with the voltage protocol shown above the traces in the absence (control) and presence of 1 μM clemizole (8 min). Clemizole had no effect on HCN4 channel current, and similar results were obtained in additional 3 sets of cells.